

# REPORT DOCUMENTATION PAGE

*Form Approved  
OMB No. 0704-0188*

for this collection of information is estimated to average 1 hour per response, including the time for reviewing instructions, searching existing data sources, gathering and maintaining the data needed, and completing and reviewing this collection of information. Send comments regarding this burden estimate or any other aspect of this collection of information, or reducing this burden to Department of Defense, Washington Headquarters Services, Directorate for Information Operations and Reports (0704-0188), 1215 Jefferson Davis Highway, Suite 1204, Arlington, VA 22202-4302. Respondents should be aware that notwithstanding any other provision of law, no person shall be subject to any penalty for failing to comply with a requirement if it does not display a currently valid OMB control number. PLEASE DO NOT RETURN YOUR FORM TO THE ABOVE ADDRESS.

E (DD-MM-YYYY)	2. REPORT TYPE Technical Papers		3. DATES COVERED (From - To)		
4. TITLE AND SUBTITLE			5a. CONTRACT NUMBER		
			5b. GRANT NUMBER		
			5c. PROGRAM ELEMENT NUMBER		
6. AUTHOR(S)			5d. PROJECT NUMBER 3058		
			5e. TASK NUMBER 00C4		
			5f. WORK UNIT NUMBER		
7. PERFORMING ORGANIZATION NAME(S) AND ADDRESS(ES)			8. PERFORMING ORGANIZATION REPORT		
Air Force Research Laboratory (AFMC) AFRL/PRS 5 Pollux Drive Edwards AFB CA 93524-7048					
9. SPONSORING / MONITORING AGENCY NAME(S) AND ADDRESS(ES)			10. SPONSOR/MONITOR'S ACRONYM(S)		
			11. SPONSOR/MONITOR'S NUMBER(S)		
12. DISTRIBUTION / AVAILABILITY STATEMENT					
Approved for public release; distribution unlimited.					
13. SUPPLEMENTARY NOTES					
14. ABSTRACT					
15. SUBJECT TERMS					
16. SECURITY CLASSIFICATION OF:			17. LIMITATION OF ABSTRACT  A	18. NUMBER OF PAGES	19a. NAME OF RESPONSIBLE PERSON Leilani Richardson
a. REPORT Unclassified	b. ABSTRACT Unclassified	c. THIS PAGE Unclassified			19b. TELEPHONE NUMBER (include area code) (661) 275-5015

Standard Form 298 (Rev. 8-98)  
Prescribed by ANSI Std. Z39-18

Item enclosed

122 035

TP-1998-142

MEMORANDUM FOR IN-HOUSE PUBLICATIONS

13 Jul 98

FROM: PROI (TI) (STINFO)

SUBJECT: Authorization for Release of Technical Information, Control Number: AFRL-PR-ED-TP-1998-142  
Keith McFall "Pulsed Thruster Thrust Stand Measurement Evaluation"  
AIAA paper (Statement A)



**AIAA-98-3805**

## **Pulsed Thruster Thrust Stand Measurement Evaluations**

K.A. McFall and G.G. Spanjers  
Propulsion Directorate  
Air Force Research Laboratory  
Edwards AFB, CA

J.H. Schilling  
Sparta, Inc.  
Propulsion Directorate  
Air Force Research Laboratory  
Edwards AFB, CA

20021122  
035

**34th AIAA/ASME/SAE/ASEE  
Joint Propulsion Conference & Exhibit  
July 12 - 15, 1998 / Cleveland, OH**

# Pulsed Thruster Thrust Stand Measurement Evaluations

Keith A. McFall\*, Gregory G. Spanjers†, John H. Schilling‡  
Propulsion Directorate, Air Force Research Laboratory  
Edwards AFB, CA 93524

This paper presents a numerical analysis of thrust stand response during pulsed thruster operation. The system model incorporates an underdamped displacement-type thrust stand under a periodic, impulsive load. Analytic and numerical methods are used to examine thrust stand measurement characteristics during simulated operation. Displacement oscillation characteristics as a function of damping coefficient ( $\alpha$ ) and the ratio ( $\tau$ ) between the time between thruster impulses and thrust stand natural period are presented. The effects of simulated thrust stand random displacement signal noise were quantified for  $\alpha=0.3$  with  $\tau$  varying from 0.1 to 0.7. These results show that measurement uncertainty due to noise decreases when  $\tau$  is increased. An analytic expression relating average thrust and average thrust stand displacement was derived. Using this expression, the effect of time-dependent, random thruster impulse variability was examined. Numerical simulations were used to estimate the dependence of thrust measurement uncertainty on the number of impulses used for averaging. These results also showed that measurement uncertainty due to impulse bit variability decreased when  $\tau$  is increased. Integration of 10 impulses is adequate to achieve measurement uncertainty below 2% for a random 10% impulse bit variation.

## NOMENCLATURE

$c_k$	= displacement coefficients
$c_k^{ideal}$	= displacement coefficients for uniform impulses
$d_k$	= fractional displacement coefficient differences: equal to $(c_k^0 - c_k^N) / c_k^{ideal}$
$f$	= fractional time within an impulse
$I_{bit}$	= thruster impulse bit
$J$	= index for counting impulses
$K$	= thrust stand spring constant
$m$	= thrust stand effective mass
$N$	= number of impulses averaged
$t$	= time
$t_p$	= thruster pulse period: time between impulses
$T_{nat}$	= natural period: equal to $2\pi / \sqrt{K/m}$
$x$	= displacement amplitude

$x_{ave}$	= time averaged displacement
$x_{max}$	= maximum displacement during impulse
$x_{min}$	= displacement at time of impulse
$y_k$	= dimensionless linear independent solution to the thrust stand equation of motion
$\alpha, \bar{\alpha}$	= damping coefficient and damping rate
$\gamma$	= fractional displacement noise
$\delta$	= fractional impulse bit variability
$\epsilon_r, \epsilon_d$	= noise and impulse induced measurement uncertainty
$\phi$	= amplitude fraction corresponding to average thrust
$\tau$	= pulse period ratio: equal to $t_p / T_{nat}$

## INTRODUCTION

The Air Force Research Laboratory is investigating the application of small satellite propulsion

\* Research Engineer, AFRL Electric Propulsion Laboratory, Member AIAA

† Group Leader, AFRL Electric Propulsion Laboratory, Member AIAA.

‡ Research Engineer, Sparta Inc., Member AIAA.

technology to support future DOD propulsion requirements<sup>1,2</sup>. NASA has evaluated the use of pulsed plasma thrusters (PPT) for the proposed third deep space mission (DS-3) of the New Millennium Program<sup>3</sup>. With the continuing interest in these and other small satellite missions<sup>4,5</sup>, propulsion system designs are being explored which use pulsed operation to achieve both high specific impulse and low power operation. An accurate measurement of thruster performance is critical for mission analysis and thruster selection.

A pulsed thruster applying an impulsive load on a displacement-type thrust stand<sup>6,7,8</sup> results in oscillations about the average displacement. When the thruster discharge frequency is much greater than the natural frequency of the thrust stand, and the discharges produce uniform (shot to shot) impulse bits, the thrust stand displacement is nearly fixed as a function of time. However, as the discharge frequency is reduced, the amplitude of the displacement oscillation increases.

Methods to accurately measure the impulse bit have included rapidly pulsed thruster operation (where the ratio ( $\tau$ ) between the time between successive impulses (thruster pulse period,  $t_p$ ) and thrust stand natural period ( $T_{nat}$ ) is very small,  $\approx 1/30$ )<sup>6</sup>, the use of single pulse impulse bit measurements<sup>6,7,8</sup>, or the use of very long period thrust stand designs<sup>8</sup>. These devices have measured impulse bits in the 100-300  $\mu\text{N}\cdot\text{s}$  range, with measurement uncertainties ranging from  $\pm 5\%$ <sup>8</sup> to less than 2%<sup>7</sup>. While these devices have demonstrated a high degree of measurement accuracy, the analytical models used to interpret the data are only strictly valid for measurements with  $\tau \ll 1$  or with a single impulse. Past modeling efforts have examined the transformation of the equations of motion for a torsional thrust stand from a rotational to a translational reference frame<sup>6</sup>, damped<sup>7</sup> and undamped<sup>9</sup> single impulse displacement, and the very long period motion of "Watt's Pendulum."<sup>8</sup>

This paper presents an analysis of the dynamic response of an under-damped displacement-type thrust stand under periodic, impulsive loads. Analytic and numerical methods are used to examine thrust stand displacement characteristics during simulated operation for a range of damping coefficients ( $\alpha$ ) and  $\tau$ . Thrust measurement approximations and accuracy are presented. The effects of simulated thrust stand displacement noise and time-dependent random thruster impulse variability are examined.

The application of a comprehensive theory of thrust stand operation under periodic, impulsive loads has the potential to provide accurate measurements over a wide range of  $\tau$ . Such a capability would allow greater flexibility in experiment design. In addition, an improved understanding of data analysis would provide an opportunity for improved accuracy, error estimation, and data reduction rates.

## THEORY OF THRUST STAND DYNAMICS

The analytical model of the thrust stand is chosen to be that of an underdamped oscillator. The general equation governing the oscillatory motion of the thrust stand under load is that of a second order damped harmonic oscillator with constant coefficients, given in Eq. 1. The displacement ( $x$ ) is a function of time ( $t$ ), damping rate ( $\bar{\alpha} = 2\sqrt{K/m} \alpha$ ), spring constant ( $K$ ), effective system mass ( $m$ ), thruster load ( $F$ ), and initial conditions for displacement and velocity.

$$x''(t) + \bar{\alpha}x'(t) + \frac{K}{m}x(t) = \frac{F(t)}{m} \quad (1)$$

The modeling effort first examines thrust stand response under uniform, periodic, impulsive load. This case is representative of an ideal system where neither the thruster, nor the thrust stand exhibits any non-uniform characteristics; the displacement data is accurate and the thruster provides a reproducible impulse bit. Representative displacement oscillations are shown in Figure 1 for three values of  $\tau$ . Equations describing thrust stand displacement as a function of time and operating parameters are presented below. Next, the effect of noisy displacement data on impulse bit calculations is examined. Finally, the relationship between measured displacement and thrust for non-uniform, periodic, impulsive loads is considered.

With the assumption of a periodic impulsive load, the oscillatory motion is dependent upon  $\alpha$ ,  $\tau$ ,  $K$ , the period between impulses ( $t_p$ ), and the thruster impulse bit ( $I_{bit}$ ). The equations governing thrust stand response then reduce to those given in Eqs. 2-4. The fractional time within an impulse,  $f$ , defines the time-wise location within a given impulse. The pulse period fraction,  $\hat{f}$ , is equal to fraction of time within the impulse that occurs after the displacement maximum (Fig. 1).  $\hat{f}$  is calculated using Eqs. 2 and 3; the displacement at  $\hat{f}$  is equal to  $x_{min}$ . Eq. 4 is used to compute the maximum thrust stand displacement ( $x_{max}$ ). Eq. 2 is used to calculate the time history of displacement, which begins with an impulse at  $f = \hat{f} - 1$ , and ends at  $f = \hat{f}$ .

$$x(f, \tau, \alpha) = x_{max} e^{-2\alpha f \pi \tau} \left( \cos\left(2\sqrt{1-\alpha^2} f \pi \tau\right) + \frac{\alpha \sin\left(2\sqrt{1-\alpha^2} f \pi \tau\right)}{\sqrt{1-\alpha^2}} \right) \quad (2)$$

$$x(\hat{f}, \tau, \alpha) = x(\hat{f}-1, \tau, \alpha) \quad (3)$$

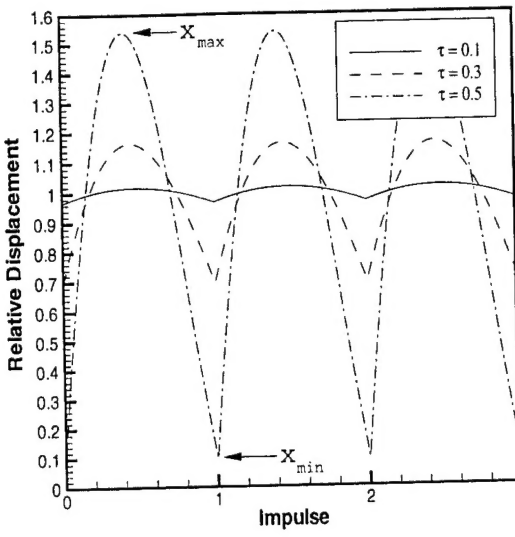


**Fig. 1 Idealized thrust stand displacement**

$$x_{\max} = \frac{I_{bit}}{K t_p} 2\pi\tau\sqrt{1-\alpha^2}$$

$$\left( \begin{array}{l} \sin(2\pi\hat{f}\sqrt{1-\alpha^2}\tau)e^{-2\pi\hat{f}\alpha\tau} + \\ \sin(2\pi(1-\hat{f})\sqrt{1-\alpha^2}\tau)e^{-2\pi(1-\hat{f})\alpha\tau} \end{array} \right)^{-1} \quad (4)$$

From the results obtained above, the displacement associated with the average thrust can be computed (Eq. 5). Eqs. 4 and 5 show that the average displacement,  $x_{ave}$ , is equal to  $\frac{I_{bit}}{K t_p}$ ; this will later be shown to be a special case of oscillator behavior.

$$x_{ave}(\hat{f}, \alpha, \tau) = \frac{x_{\max} \left( \begin{array}{l} \sin(2\pi\hat{f}\sqrt{1-\alpha^2}\tau)e^{-2\pi\hat{f}\alpha\tau} + \\ \sin(2\pi(1-\hat{f})\sqrt{1-\alpha^2}\tau)e^{-2\pi(1-\hat{f})\alpha\tau} \end{array} \right)}{2\pi\sqrt{1-\alpha^2}\tau} \quad (5)$$

#### A. Displacement Noise

The effect of displacement data noise on impulse bit calculations is examined through the addition of random noise to the ideal displacement curves described by Eqs. 2-4. Displacement noise is computed using a random amplitude with standard deviation equal to a

fractional error,  $\gamma$ , multiplied by the amplitude of maximum displacement. The resulting displacement data is analyzed using a commercial non-linear fitting algorithm<sup>10</sup>. A modified version of Eq. 2, which allows for shifts in time of maximum displacement, is the fitted to the data. The algorithm fits four independent parameters and computes the  $\alpha$ ,  $\tau$ ,  $\hat{f}$ ,  $x_{max}$ , then  $I_{bit}$  for each impulse.

#### B. Non-Uniform Impulse Loads

The effect of non-uniform, periodic, impulsive loads on average thrust calculations is examined. This analysis assumes that disturbance forces, the effect of noise, and drift associated with thrust stand measurement are negligible. A transient solution to Eq. 1 was implemented, with the impulse bit for each pulse computed using a random addition to the average with a standard deviation equal to a fractional variation,  $\delta$ , from the average (Fig. 2). An analytic solution for displacement under non-uniform, periodic, impulsive load was derived. The general solution for damped oscillator<sup>11</sup> motion is given in Eqs. 6-8. The recursion relation for the fitting parameters (Eqs. 9-10) was derived for an underdamped thrust stand. The parameter  $f$  again describes the dimensionless time within an impulse cycle of duration  $t_p$ . For this case,  $f$  varies from 0 to 1. Impulses are numbered by the index  $J$  in parenthesis. The first derivative term in Eq. 10 is with respect to the dimensionless parameter  $f$ .

$$x(c_1, c_2, f) = c_1 y_1(\alpha, \tau, f) + c_2 y_2(\alpha, \tau, f) \quad (6)$$

$$y_1(\alpha, \tau, f) = e^{-2\alpha\tau\pi f} \cos\left(2\sqrt{1-\alpha^2}f\pi\tau\right) \quad (7)$$

$$y_2(\alpha, \tau, f) = e^{-2\alpha\tau\pi f} \sin\left(2\sqrt{1-\alpha^2}f\pi\tau\right) \quad (8)$$

$$c_1^{(J)} = x(c_1^{(J-1)}, c_2^{(J-1)}, 1) \quad (9)$$

$$c_2^{(J)} = \left\{ \begin{array}{l} \dot{x}(c_1^{(J-1)}, c_2^{(J-1)}, 1) + \frac{I_{bit}^{(J)}}{K} \left( \frac{2\pi\tau}{t_p} \right)^2 t_p + \\ \frac{2\pi\alpha\tau x(c_1^{(J-1)}, c_2^{(J-1)}, 1)}{2\pi\tau\sqrt{1-\alpha^2}} \end{array} \right\} \quad (10)$$

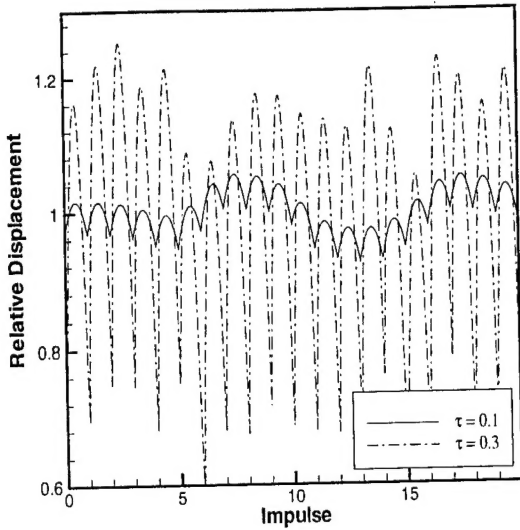


**Fig. 2 Simulated thrust stand displacement with impulse bit variance ( $\delta = 0.05$ )**

Eqs. 6-10 were examined analytically to determine the relationship between the average displacement and the average impulse bit ( $I_{bit}^{ave} = \frac{1}{N} \sum_{J=1}^N I_{bit}^J$ ) for an impulse set of  $N$  impulses. The recursion relation is solved using a summation and matrix inversion technique. It is found that the impulse induced displacement uncertainty ( $\tilde{\varepsilon}_d$ ), the fractional difference between the measured average displacement ( $x^{ave}$ ) and the displacement associated with the average thrust ( $I_{bit}^{ave} / t_p$ ), is equal to Eq. 12; equation simplification was accomplished using commercial symbolic mathematical manipulation routines<sup>12</sup>. The parameter  $d_1$  and  $d_2$  are defined in Eqs. 13-15.  $d_k$  equals the difference between the beginning and ending coefficients divided by  $c_k^{ideal}$ , the value for uniform impulses ( $\delta=0$ ). Thus, when the starting and ending displacement curves are equal, as is the case for uniform periodic impulses, the average displacement is equal to the displacement associated with the average thrust.

$$\tilde{\varepsilon}_d = \frac{x^{ave} - \left( \frac{I_{bit}^{ave}}{K t_p} \right)}{\left( \frac{I_{bit}^{ave}}{K t_p} \right)} \quad (11)$$

$$\tilde{\varepsilon}_d = \frac{\left[ d_2 e^{2\alpha\tau\pi} \cos\left(2\sqrt{1-\alpha^2}\pi\tau\right) + \frac{(d_1-d_2)}{2} \cos\left(4\sqrt{1-\alpha^2}\pi\tau\right) + \left[ -\frac{(d_1+d_2)}{2} + \frac{\alpha}{\sqrt{1-\alpha^2}} d_2 e^{2\alpha\tau\pi} \sin\left(2\sqrt{1-\alpha^2}\pi\tau\right) + \frac{\alpha}{\sqrt{1-\alpha^2}} \frac{d_1-d_2}{2} \sin\left(4\sqrt{1-\alpha^2}\pi\tau\right) \right] \right]}{N \left( 1 + e^{4\alpha\tau\pi} - 2e^{2\alpha\tau\pi} \cos\left(2\sqrt{1-\alpha^2}\pi\tau\right) \right)} \quad (12)$$

$$d_k = \frac{c_k^0 - c_k^N}{c_k^{ideal}} \quad (13)$$

$$c_1^{ideal} = \frac{\left( 2\pi\tau I_{bit}^{ave} \sin\left(2\sqrt{1-\alpha^2}\pi\tau\right) \right)}{\left( \sqrt{1-\alpha^2} K t_p \left( e^{2\alpha\tau\pi} + e^{-2\alpha\tau\pi} - 2\cos\left(2\sqrt{1-\alpha^2}\pi\tau\right) \right) \right)} \quad (14)$$

$$c_2^{ideal} = \frac{2\pi\tau I_{bit}^{ave} \left( 1 - e^{-2\alpha\tau\pi} \cos\left(2\sqrt{1-\alpha^2}\pi\tau\right) \right)}{\left( \sqrt{1-\alpha^2} K t_p \left( 1 + e^{-4\alpha\tau\pi} - 2e^{-2\alpha\tau\pi} \cos\left(2\sqrt{1-\alpha^2}\pi\tau\right) \right) \right)} \quad (15)$$

This analysis proves that, subject to the model assumptions, average displacement measurements approximate the displacement associated with average thrust to an accuracy that is inversely proportional to the number of impulse bits averaged. Also,  $\tilde{\varepsilon}_d$  is equal to zero for any set of impulses for which the first and last displacement histories are the same.

## NUMERICAL ANALYSIS

The displacement ( $\frac{I_{bit}}{K t_p}$ ) associated with the average thrust relative to  $x_{max}$  and  $x_{min}$  is represented by the thrust coefficient ( $\phi$ ) (Eq. 16). The values for  $x_{max}$  and  $x_{min}$  are calculated using Eq. 2 for  $f = 0$  and  $f = \hat{f}$ , respectively. By characterizing  $\phi$  for a range of damping coefficients and pulse period ratios, the displacement associated with average thrust can be computed accurately with the measurement of  $x_{max}$ ,  $x_{min}$ ,  $\alpha$ , and  $\tau$ . Using Eqs. 2-5,  $\phi$  was calculated as a function of  $\alpha$  and  $\tau$  (Fig. 3). The figure shows that the thrust coefficient varies only slightly for pulse period ratios less than 0.5.

$$\phi(\alpha, \tau) = \frac{\frac{I_{bit}}{K t_p} - x_{min}}{x_{max} - x_{min}} \quad (16)$$

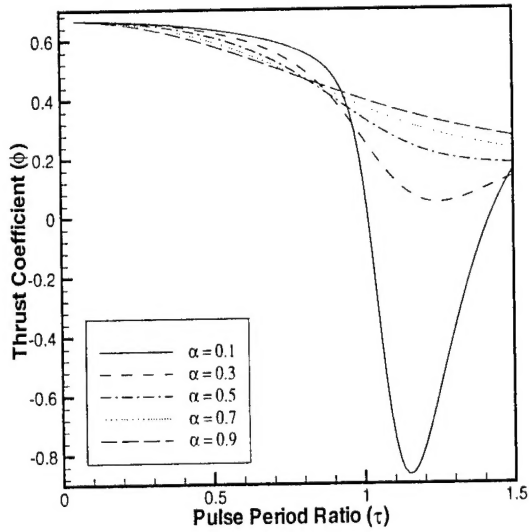


Fig. 3 Thrust coefficient as a function of  $\alpha$  and  $\tau$

For the special case of undamped oscillation, a simple expression exists for  $\phi$  (Eq. 17). When this analytic expression is used to compute  $\frac{I_{bit}}{K t_p}$ , the fractional error in impulse bit resulting from the approximation is less than 2% for pulse periods approaching 0.4 (Fig. 4).

$$\phi(0, \tau) = \frac{\frac{1}{\pi\tau} \sin(\pi\tau) - \cos(\pi\tau)}{1 - \cos(\pi\tau)} \quad (17)$$

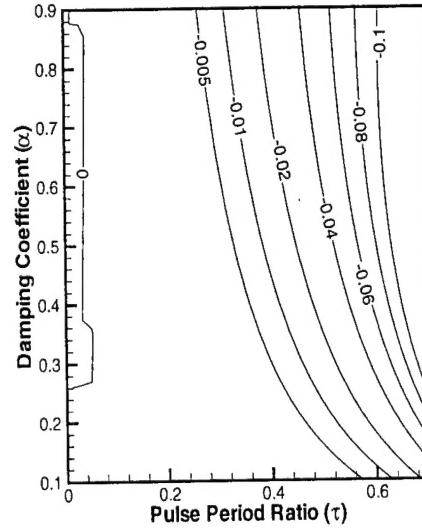
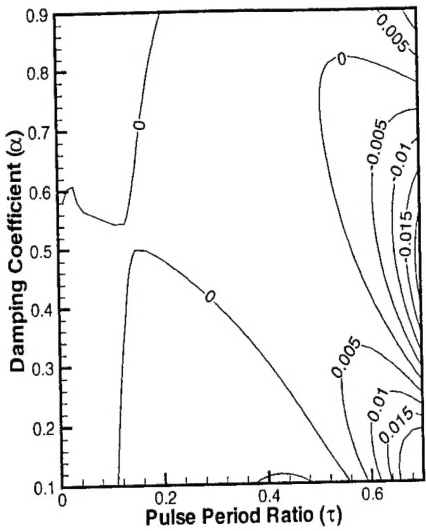


Fig. 4 Fractional thrust error with assumption of no damping

An improved approximation for  $\phi$  was determined using Eq. 17 as the first term in a functional expansion. Calculated values of  $\phi$  were used to determine a polynomial fit to the expression. A 36 by 36 matrix of calculated values for  $\alpha$  (0.1-0.9) and  $\tau$  (0.01-0.7) provided the input to the regression algorithm<sup>10</sup>. The fitted function includes first and second order terms. The resulting expression is given below:

$$\begin{aligned} \phi(\alpha, \tau) &= \phi(0, \tau) + \\ &(-0.0098881 + \alpha(0.014532) + \tau(0.11039) + \\ &\alpha\tau(-0.17889) + \alpha^2(0.0042004) + \tau^2(-0.14525)) \end{aligned} \quad (18)$$

This expression provides a significant improvement in accuracy over the strictly analytic approximation. Use of this approximation provides a thrust error less than 2% for all values of  $\alpha$  and  $\tau$  shown in Fig. 5.



**Fig. 5** Fractional thrust error with second order polynomial approximation

## ERROR ANALYSIS RESULTS

This paper examines the thrust measurement uncertainties associated with two types of error sources: random noise and non-uniform impulse bit sets. To evaluate the magnitudes associated with these error sources, two different analysis methods were used. Displacement uncertainty associated with noisy thrust stand displacement data was analyzed by fitting simulated random thrust stand displacement perturbations. The effect of non-uniform impulse bit thruster operation is evaluated using numerical simulation and the analytic expression for thrust measurement error given in Eq. 12.

### A. Displacement Noise

Displacement noise perturbation magnitude was varied from zero to  $4.0 \times 10^{-3}$  times the peak oscillation amplitude for each case. The factor  $\gamma$  is the fractional magnitude (standard deviation) of the noise with respect to peak oscillation amplitude. Results from the fitting of 50 impulses for each condition are shown in Fig. 6. For all cases, a damping coefficient of 0.3 was used. The displacement uncertainty for noisy displacement data,  $\epsilon_\gamma$ , is defined as the standard deviation of the set of fractional differences between the fitted and exact impulse bits (Eq. 19). The fitted impulse bit is computed using Eq. 5 and the fitted values for  $\alpha$ ,  $\tau$ ,  $\hat{f}$ , and  $x_{max}$ . The fitting of the damping coefficient was seen to depend strongly on  $\tau$ , with standard deviation variations of more than 100% above the average resulting for  $\tau = 0.1$  compared to

around 5% for  $\tau = 0.3$ . These results are consistent with the increase in the effect of damping at large values of  $\tau$ , and the anticipated sensitivity to noise associated with small values of  $\tau$  where damping is less of a perturbing force. No significant influence of  $\tau$  on the other fitting variables was observed. For all cases examined, the average value for the differences was at least two orders of magnitude less than the standard deviation, indicating that the effect of random noise is distributed evenly about the exact value.

$$\epsilon_\gamma = \text{Std dev} \left( \frac{I_{bit}^{J; \text{calc}} - I_{bit}^{\text{exact}}}{I_{bit}^{\text{exact}}} \right) \quad (19)$$

The results show that  $\epsilon_\gamma$  decreases as the pulse period increases within the range from 0.1 to 0.3. This effect is consistent with the large variability in calculated values of  $\alpha$  for small values of  $\tau$ . Within the region between  $\tau = 0.3$  and 0.7, where  $\alpha$  is less variable,  $\epsilon_\gamma$  is approximately constant.

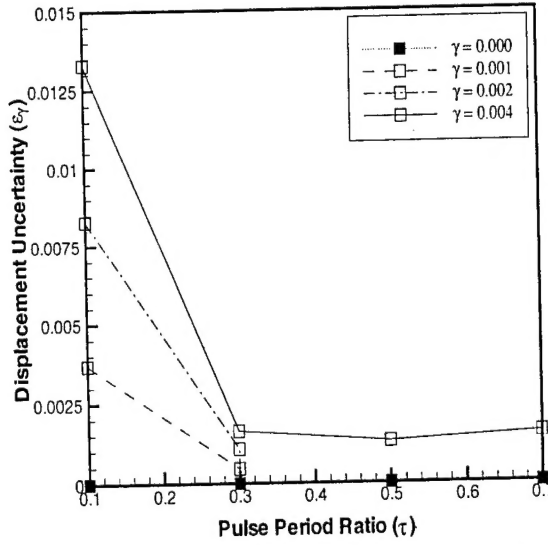


**Fig. 6** Displacement uncertainty for noisy displacement data ( $\alpha = 0.3$ )

In addition to the  $\alpha = 0.3$  results, additional calculations were made for  $\alpha = 0.7$ ,  $\tau = 0.1$ . At this high level of damping, the larger variability of calculated values of  $\alpha$  was also observed for  $\tau = 0.1$ . Though the calculated value of  $\epsilon_\gamma$  did not differ significantly from the results shown in Fig. 6, the number of iterations required to produce a converged solution increased significantly from that observed for  $\alpha = 0.3$  (from about 10 to over 100). This is consistent with the large variability in the fitted value of  $\alpha$ , which results in values of  $\alpha$  that exceed unity, the range of applicability of the equations used to model thrust stand response.

## B. Non-Uniform Impulse Loads

The effect of non-uniform impulse bits on thrust measurement was evaluated numerically using Eq. 12 and numerical simulations of thrust stand response. The measurement uncertainty,  $\epsilon_d$ , associated with randomly variable impulse bit is calculated from the standard deviation of a set of  $\tilde{\epsilon}_d$  values. The parameter  $d_1$  and  $d_2$  are calculated for each impulse; a first order examination of the distribution of these parameters confirmed that they are equally distributed about  $d_k = 0$ . For the results presented in Figs. 7 and 8, each point was the result of 100 data sets. The dependency of  $\epsilon_d$  on  $\alpha$  and  $\tau$  is presented in Fig. 7. For these cases, the impulse sets consisted of 5 impulses ( $N=5$ ) and the impulse bit standard deviation ( $\delta$ ) is 5%. These results show that, in general,  $\epsilon_d$  decreases with increasing  $\alpha$  and  $\tau$ ; though the  $\alpha = 0.7$  data conflicts somewhat with this conclusion, the limited sampling sizes used can explain such a discrepancy (discussed below). The largest variation occurs for  $\alpha$  and  $\tau$  between 0.1 and 0.3.

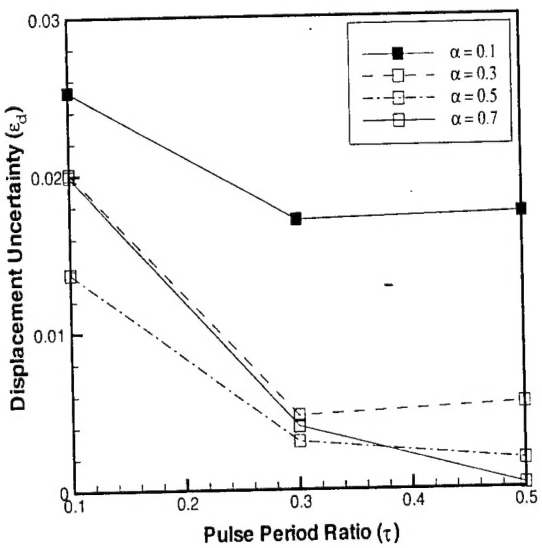


Fig. 7 Displacement measurement uncertainty for non-uniform periodic impulse bits (5% standard deviation variability, 5 impulses per pulse set, 100 sets)

The effect of impulse set length and impulse bit variability is shown in Fig. 8. As expected from Eq. 12, the results show a near inverse relation between  $\epsilon_d$  and  $N$ . In addition,  $\epsilon_d$  is approximately proportional to impulse variability ( $\delta$ ). These results show that thrust measurements using integrated displacement data can accurately represent the average thrust for even relatively small impulse set sizes. For example, the integration of 10

impulses is sufficient to provide a less than 2% measurement standard deviation for a random 10% impulse bit standard deviation.

Based on calculations with large sampler sizes (200, 400, and 800) compared to the 100 used for the results shown in Fig. 7 and 8, the accuracy of the data presented is estimated to be within 50%. An accuracy of that magnitude is consistent with the relative location of the  $\alpha = 0.7$  line in Fig. 7.

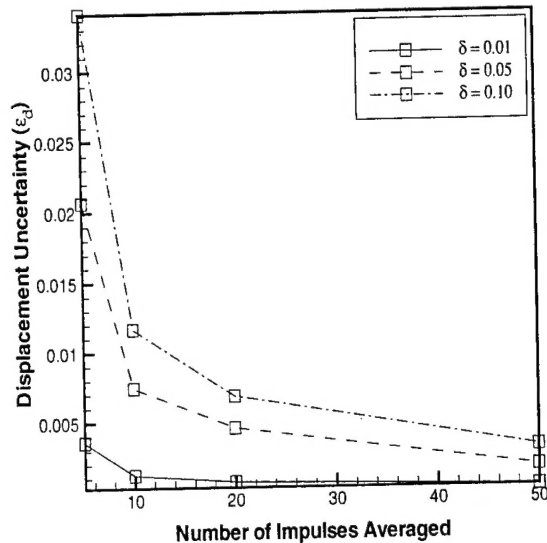


Fig. 8 Displacement measurement uncertainty for non-uniform periodic impulse bits ( $\alpha = 0.3$ ,  $\tau = 0.1$ )

## DISCUSSION

The analytic examination of thrust stand dynamics provides sensitivity estimates for thrust stand measurement accuracy as a function of data reduction method. The results presented show the relative sensitivity of thrust stand accuracy on damping and the ratio between pulse period and thrust stand natural (undamped) period.

The data show that the uncertainty associated with random displacement noise decreases as the pulse period ratio,  $\tau$ , is increased when a curve fitting technique is used to calculate individual impulse bits; this effect is greatest for  $\tau < 0.3$ . This technique also experiences convergence difficulties when  $\alpha$  approaches unity.

An analytic expression for measurement accuracy was derived for an underdamped thrust stand under non-uniform period impulsive loading. This expression provides a means of estimating the uncertainty associated with a very simple method of thrust measurement analysis, the averaging of thrust stand

displacement. This analysis indicates that measurement uncertainties associated with relatively large impulse bit variability can be reduced through the integration of a relatively small number of impulses, on the order of 10. With such a small number of impulses required to accurately determine average thrust, it is believed that this method would be applicable for the analysis of even transient effects, such as the rapid increase in thruster impulse bits due to discharge energy change. In addition, data analysis is expected to be very rapid due to simplicity of the numerical technique; the displacement data is averaged with respect to time. The data also show that measurement uncertainty decreases as  $\tau$  is increased; this effect is greatest for  $\tau < 0.3$ .

The approximations used in the displacement averaging thrust measurement technique are believed to accurately represent the thrust stand system. While random and periodic disturbances are omitted from the analysis, it is anticipated that they will largely cancel provided that their period of oscillation is much less than the averaging period. Displacement drift is not expected to be a significant source for measurement uncertainty provided it remains linear over the duration required for displacement averaging.

Two issues remain that will require experimental confirmation to determine their significance. The first is non-random electromagnetic induced displacement noise. Effective shielding of data acquisition electronics is expected to adequately address this problem. The second issue is that of the assumption of constant coefficients in the second order differential equation. While not expected to be an issue, the derivation is only exact if the coefficients are constant. It is anticipated that the accuracy of the technique can be confirmed through the comparison of thrust analysis results for a range of pulse period ratios. Variation of both thruster pulse period and thrust stand natural period would be used.

An interesting conclusion that can be drawn from this analysis is that there is an accuracy advantage associated with the use short period ( $\tau > 0.3$ ) thrust stand designs. With  $\tau$  proportional to  $\sqrt{K/m}$ , this indicates that more accurate measurements can be obtained using less massive (also more compact, since  $m$  is proportional to the thrust stand moment of inertia<sup>6</sup>) thrust stands. Such systems could be used in smaller vacuum chambers and, due to their reduced size, would be simpler to mechanically isolate. A small, well isolated, high accuracy thrust stand could provide a means of accurately measuring impulse bits in the sub-100 $\mu$ N-s range.

## SUMMARY

This paper presents a numerical analysis of thrust stand response during pulsed thruster operation. A summary of the results is given below:

- Displacement oscillation shape as a function of  $\alpha$  (0.1 to 0.9), and  $\tau$  (0.05 to 1.5) are presented. Impulse approximation techniques accurate to within 2% for  $\tau$  less than 0.7 are shown.
- Displacement signal noise effects were quantified for  $\alpha=0.3$  with  $\tau$  varying from 0.1 to 0.7. Thrust measurement uncertainties below 2% result from fractional noise amplitudes less than 0.004. Measurement uncertainty due to noise decreases when  $\tau$  is increased to  $\sim 0.3$ .
- An analytic expression relating average thrust and integrated thrust stand displacement was derived. Numerical simulations were used to estimate thrust uncertainty dependence on the number of impulses used for averaging. Measurement uncertainty due to impulse bit variability decreases when  $\tau$  is increased to  $\sim 0.3$ . Integration of 10 impulses is adequate to achieve measurement uncertainty below 2% for a random 10% impulse bit variation.

---

<sup>1</sup> Tilley, D.L., et al., "Life Extension Strategies for Shuttle-Deployed Small Satellites Using Pulsed Plasma Thrusters," *Journal of Spacecraft and Rockets*, Vol. 34, No. 6, November-December 1997, pp. 785-791.

<sup>2</sup> Spores, R.A., et al., "The Air Force Electric Propulsion Program," AIAA Paper 98-3181, July 1998.

<sup>3</sup> Blandino, J.J., "Pulsed Plasma Thrusters for the New Millennium Interferometer (DS-3) Mission," IEPC Paper 97-192, August 1997.

<sup>4</sup> Rudikov, A.I., et al., "Pulsed Plasma Thruster of the erosion type for a geostationary artificial earth satellite," *Acta Astronautica*, Vol. 35, No. 9-11, 1995, pp. 585-590.

<sup>5</sup> Choueiri, E.Y., "System Optimization of Ablative Pulsed Plasma Thrusters for Stationkeeping," *Journal of Spacecraft and Rockets*, Vol. 33., No. , January-February 1996, pp. 96-100.

<sup>6</sup> Haag, T.W., "Thrust stand for pulsed plasma thrusters," *Rev. Sci. Instru.*, Vol. 68, No. 5, May 1997, pp. 2060-2067.

<sup>7</sup> Cubbin, E.A., et al., "Pulsed thrust measurements using laser interferometry," *Rev. Sci. Instru.*, Vol. 68, No. 6, June 1997, pp. 2339-2346.

<sup>8</sup> Wilson, M.J., et al., "A Compact Thrust Stand for Pulsed Plasma Thrusters, IEPC paper 97-122, August 1997.

<sup>9</sup> Paccani, G., "Quasisteady Ablative Magnetoplasmadynamic Thruster Performance with Different Propellants," *Journal of Propulsion and Power*, Vol. 14, No. 2, March-April 1998, pp. 254-260.

<sup>10</sup> *Mathematica 3.0 Standard add-on packages*, Wolfram Media, 1996.

<sup>11</sup> *Elementary Differential Equations (Third Edition)*, John Wiley & Sons, 1977.

<sup>12</sup> *Mathematica 3.0*, Wolfram Research, 1996.